

Article

Evaluation of Cloud Water Resources in the Huaihe River Basin Based on ERA5 Data

Jinlan Gao, Jingjing Feng, Yanan Cao * and Xiaoyi Zheng

Anhui Weather Modification Office, Heifei 230031, China; gaojinlan87@126.com (J.G.); fjj1018@163.com (J.F.); xyzheng@mail.ustc.edu.cn (X.Z.)

* Correspondence: cyn@mail.ustc.edu.cn

Abstract: High-resolution reanalysis data are an effective way to evaluate cloud water resources (CWRs). Based on ERA5 reanalysis data and gridded observed precipitation data, combined with the diagnostic quantification method of cloud water resource (CWR-DQ), we analyze and evaluate the CWRs and their distribution characteristics in the Huaihe River Basin from 2011 to 2021. Moreover, we compare and evaluate the CWRs of two typical precipitation processes in summer and winter. The results show that the annual total amount of atmospheric hydrometeor (GM_h) in the Huaihe River Basin is approximately 1537.3 mm. The precipitation (P_s) is 963.5 mm, the cloud water resource (CWR) is 573.8 mm, and the precipitation efficiency of hydrometeor (PE_h) is 62.4%. The CWR in the Huaihe River Basin shows a slow increasing trend from 2011 to 2021. The monthly variations in P_s , CWR, and PE_h show a single peak distribution. The spatial horizontal distributions of the gross mass of water vapor (GM_v), GM_h , and P_s in the Huaihe River Basin are zonal, and the values decrease with increasing latitude. In summer, the hydrometeors are mainly distributed in the middle layer (between 600 and 350 hPa). The hydrometeors in spring, autumn, and winter are mainly below 500 hPa. Two cases reveal that GM_v , the condensation from water vapor to hydrometeors (C_{vh}), GM_h , P_s , and PE_h in the summer case are significantly higher compared to those in the winter case, while the CWRs are similar. The results are helpful for proposing rational suggestions for the Huaihe River Basin and to provide some beneficial reference for the development of CWRs.

Keywords: ERA5; cloud water resources (CWRs); spatiotemporal distribution; evaluation analysis; Huaihe River Basin



Citation: Gao, J.; Feng, J.; Cao, Y.; Zheng, X. Evaluation of Cloud Water Resources in the Huaihe River Basin Based on ERA5 Data. *Atmosphere* **2023**, *14*, 1253. <https://doi.org/10.3390/atmos14081253>

Academic Editor: Kui Chen

Received: 27 June 2023

Revised: 30 July 2023

Accepted: 3 August 2023

Published: 7 August 2023



Copyright: © 2023 by the authors. Licensee MDPI, Basel, Switzerland. This article is an open access article distributed under the terms and conditions of the Creative Commons Attribution (CC BY) license (<https://creativecommons.org/licenses/by/4.0/>).

1. Introduction

In the context of global warming, ecological problems involving resources and the environment are becoming increasingly prominent in China, and disaster prevention and mitigation situations are very serious [1–4]. The plain area of the Huaihe River Basin occupies nearly 67% of the total area, grain yields occupy nearly 17% of the country, and the supply of commodity grain occupies approximately 25% of the country, which is one of the important agricultural bases in China. The Huaihe River Basin is uniquely located in the northern and southern geographical boundary and climate transition zone. The climate is complex and variable, resulting in frequent droughts and floods that change rapidly. Climate problems and extreme hydrological phenomena in the river basin have been widely considered by many scholars [5–9]. Wang et al. [10] found that the inter-annual variation of extreme precipitation is remarkable over the Huaihe River Basin. Precipitation extremes in each season show an increasing trend, with their intensity also increasing [11]. The occurrence timing of extreme precipitation in the Huaihe River Basin mainly concentrates on July [12]. Higher precipitation has occurred in the south of the basin, while lower precipitation has occurred in the north of the basin [13,14]. These studies provide an important reference for understanding the climatic characteristics of precipitation in the Huaihe River Basin. In recent years, the research of CWRs has started

to be the concern of more and more scholars. In a broad sense, atmospheric cloud water resources refer to the total amount of liquid water and solid water in the atmosphere. Artificial weather modification precipitation (snow) enhancement operations are concerned with atmospheric water resources as solid or liquid particles of cloud water formed by atmospheric motion, which is the focus of many studies [15–17]. However, the main physical quantity of atmospheric water resources is reflected by cloud water content. Spatiotemporal distribution characteristics and variations in cloud water content can provide some reference for artificial precipitation enhancement [18,19]. Therefore, it is of great practical significance to improve the efficiency of weather modification services and scientifically evaluate and develop cloud water resources (CWRs) in the region.

At present, the study of CWRs is mostly based on ground-based remote sensing data [20–22], satellite data [23–25] and reanalysis data [15,26,27]. Scholars have used ground-based microwave radiometers to retrieve precipitable water vapor and path-integrated cloud liquid water [28]. Based on MODIS data, the cloud optical thickness and cloud effective radius are retrieved, and the cloud liquid water path algorithm is improved [29,30]. The vertical and regional variation characteristics of cloud water content in summer over China was analyzed based on CloudSat satellite data [31]. It showed that monthly average liquid water content at a height of 4 to 7 km in the central region is significantly higher than that in the southern and northern regions. This is due to the influence of the topography of the Qinghai-Tibet Plateau. Compared to ground-based remote sensing data and satellite data, reanalysis data have the advantages of wide coverage, high spatiotemporal resolution, good time continuity, long time series, and good consistency [32]. An increasing number of scholars have carried out research on CWRs based on reanalysis data. Liu et al. [33] used ERA-Interim reanalysis data to analyze the spatiotemporal distribution characteristics and variation trends of cloud water in China from 1979 to 2016 and found that the interannual variation in summer was much smaller than that in other seasons, and the spatial variation in cloud water showed a trend of increasing in the west and decreasing in the east. Zhang et al. [34] analyzed the spatiotemporal distribution characteristics of cloud liquid water content and cloud ice water content in Qinghai from 2009 to 2018 based on ERA-interim reanalysis data and revealed that both cloud liquid water content and cloud ice water content increased from the northwest to southeast. For the vertical distribution of cloud water, the cloud liquid water content and cloud ice water content first increased and then decreased with increasing altitude. Zhang et al. [15] found that the CWRs in Guangxi were characterized by seasonal variation based on ERA5 reanalysis data, and the maximum value of the horizontal distribution of hydrometeors appeared in northeastern Guangxi and gradually decreased to the west and south.

It is common to carry out CWRs research in the Huaihe River Basin based on ground-based remote sensing and satellite observation data (Figure 1). As early as 1998 and 1999, the Huaihe River Basin Experiment (HUBEX) in China was an important part of the Global Energy and Water Cycle Experiment/Global Atmospheric Watch Cloud and Aerosol Experiment (GEWEX/GAME). Cloud liquid water became a new research focus based on ground-based remote sensing and satellite observations [35]. Many scholars have evaluated CWRs based on HUBEX. Yao et al. [36] revealed a process of obvious increase in the amount of water vapor and cloud liquid water before the precipitation, and a process of obvious decrease after the precipitation. The cloud liquid water, precipitation cloud model, rainfall area, and rain rate were retrieved [37]. Furthermore, Cao et al. [38] found that the occurrence probability of water clouds is greater than that of ice clouds, clear sky, and mixed-phase clouds in summer. Zheng et al. [39] found that the low probability of precipitation shows an increasing trend with increases in the cloud optical depth, liquid water path, and ice water path. However, based on reanalysis data, limited research on CWRs in the Huaihe River Basin has been done.

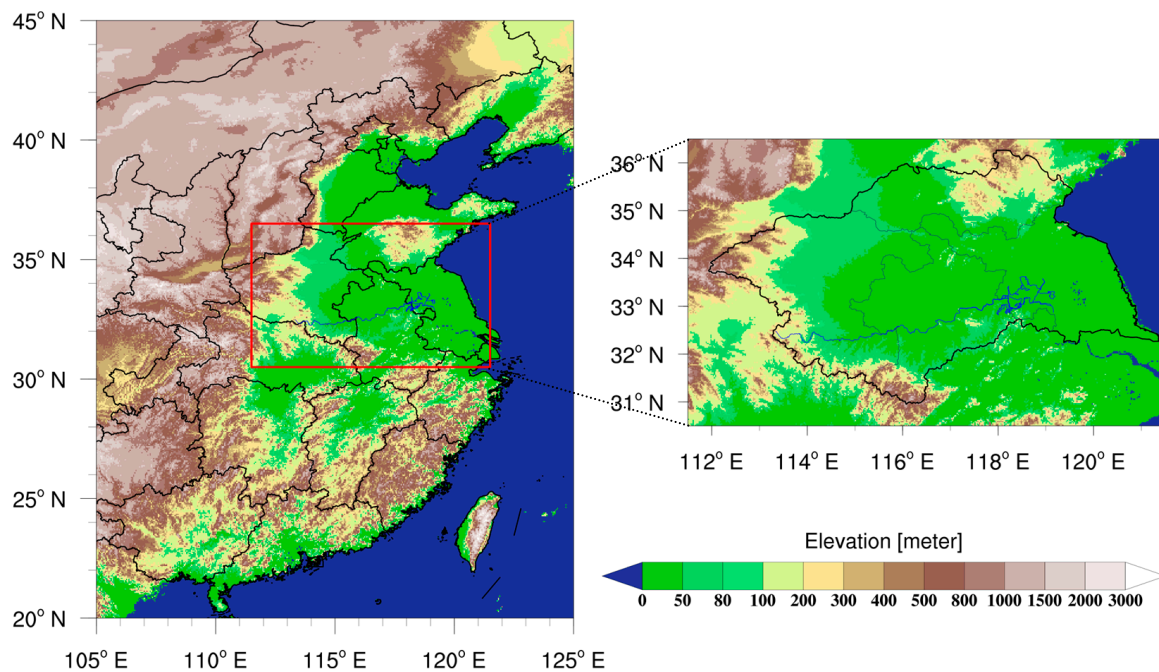


Figure 1. Location of the Huaihe River Basin in China.

Based on all of the studies above, it can be concluded that there are regional differences in CWRs among different regions due to geographical and climatic conditions. Therefore, long time scales and high-resolution reanalysis data can be used to evaluate CWRs in different regions of China, which is of great significance for further understanding the regional variation and recognition of CWRs. Based on the NCEP reanalysis data and combined with satellite data to diagnose cloud water volume, the monthly and annual CWR, related variables, and CWR characteristics of different regions in China and its six regions were analyzed using the CWR-DQ [40]. However, the reanalysis data used in their study had a rough resolution and did not have the quantities associated with cloud water, such as cloud water, cloud ice, rain, snow, etc. More detailed cloud and precipitation parameterization schemes are adopted by the ECMWF's integrated forecast system (IFS), outputting five predictands of cloud water, cloud ice, rain, snow, and cloud fraction, with a spatial resolution of 0.25° . The Huaihe River Basin is regarded as an important agricultural bases in China. At present, research based on ERA5 high-resolution reanalysis data on the precise evaluation of CWRs is rare in the region. In this study, based on ERA5 high-resolution reanalysis data and precipitation data, the CWRs in the Huaihe River Basin are evaluated for quantitative diagnosis to study the characteristics and regularities of the change. The research results can provide a useful reference for the scientific and reasonable development of CWRs in the Huaihe River Basin.

2. Materials and Methods

2.1. Data Sources

ERA5 is the fifth-generation global atmospheric reanalysis data released by the European Centre for Medium-Range Weather Forecasts (ECMWF), with a horizontal resolution of $0.25^\circ \times 0.25^\circ$, 37 vertical levels from 1000 to 1 hPa, and a time resolution of 1 h. Uniform and high spatiotemporal resolution cloud water data can be provided by ERA5 for the evaluation of CWRs. ECMWF's integrated forecast system (IFS) CY41R2 model 4D-Var data assimilation method achieves a time resolution of 1 h for data, and more detailed evolution process data can be provided for cloud and precipitation processes with rapid development. More detailed cloud and precipitation parameterization schemes are adopted by this system, improved from the previous generation ERA-Interim's two predictands of cloud water/ice and cloud fraction to five predictands of cloud water, cloud ice, rain, snow, and

cloud fraction (as shown in Figure 2). Physically, the system can more realistically reflect the main processes of cloud and precipitation generation and disappearance, including cumulus convection, condensation, sublimation, evaporation, collision, melting, freezing, and other mechanisms to form clouds [41]. ERA5 provides a large number of elements. The variables used in this study, such as wind [42,43] and evaporation [44], have been evaluated by numerous scholars. These conclusions confirm the reliability of the ERA5 dataset.

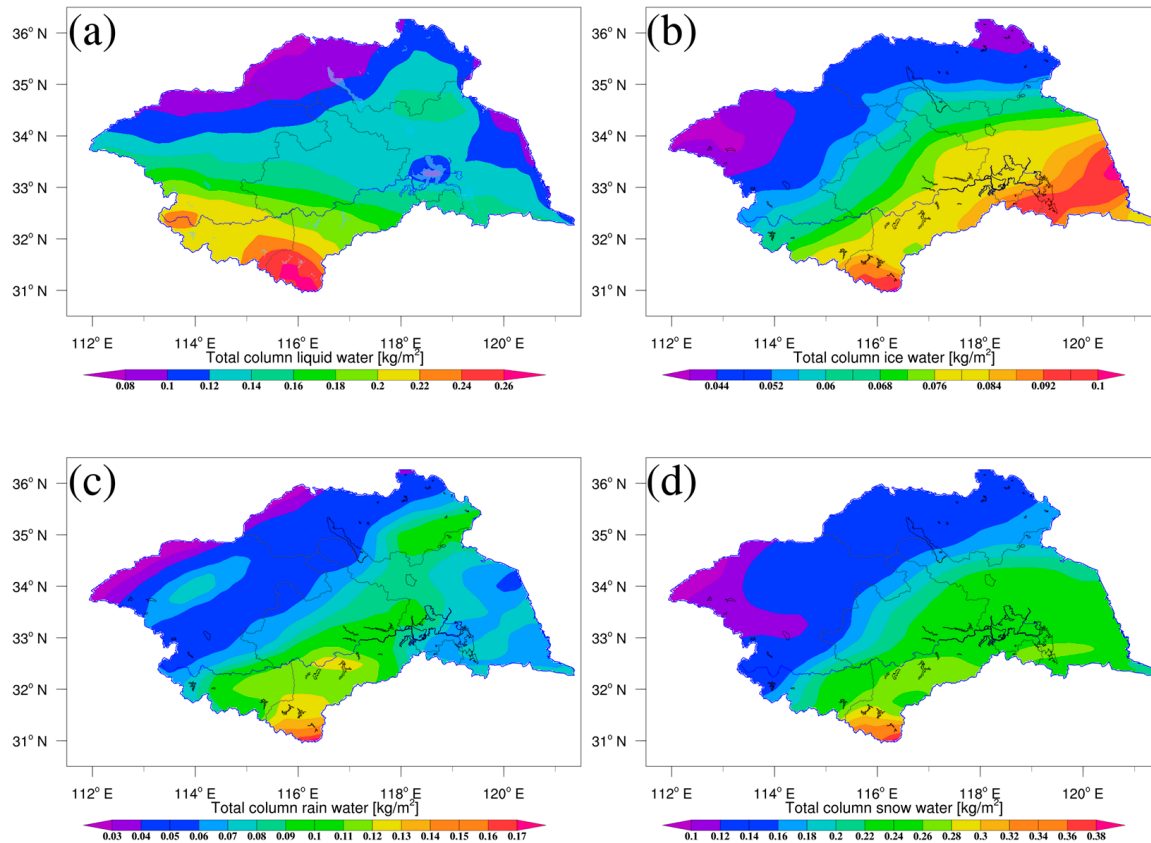


Figure 2. Cloud liquid water (a), cloud ice water (b), rain (c), snow (d) in July 2020.

The surface precipitation data were from the CN05.1 gridded precipitation observation dataset developed by the National Climate Center, with a spatial resolution of 0.25° and a daily time resolution.

2.2. Regional Boundary Processing Method

In this study, based on the horizontal spatial resolution of the ERA5 reanalysis data ($0.25^\circ \times 0.25^\circ$), the region is divided into irregular polygons composed of several $0.25^\circ \times 0.25^\circ$ grids. The CWRs in the Huaihe River Basin are calculated in a $0.25^\circ \times 0.25^\circ$ grid. For the whole area, the advection of atmospheric water substances only exists along the boundary, while the advection within the region cancels each other out. After grid processing, the left and right boundaries of the outermost grids are the west boundary and the east boundary at this latitude, respectively. For each latitude, the west boundary and east boundary can be obtained. The meridional outward boundaries of the region can be determined. The zonal outward boundaries of the region are obtained in the same way. Finally, the grids and the outer boundaries of the study area can be determined to process each grid point and calculate the input and output on the boundary. The boundary and grid processing methods of the Huaihe River Basin are shown in Figure 3. In the figure, green, blue, and dark blue represent the advection transport of hydrometeors through one, two, and three boundaries of the grid, respectively.

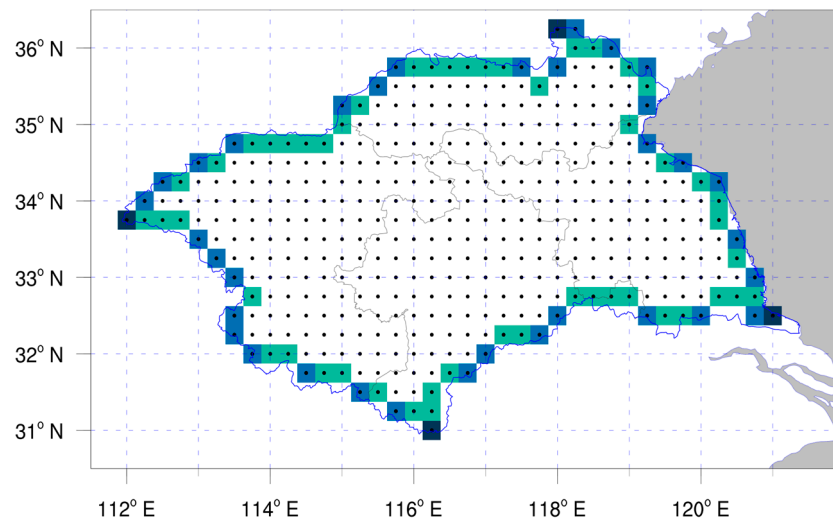


Figure 3. Schematic diagram of the boundary gridding process in the Huaihe River Basin.

2.3. Research Methods

The evaluation method is regarded as the main framework based on diagnostic quantification of the cloud water resource (CWR-DQ), which was released by the weather modification center of the China Meteorological Administration [45,46]. In this study, the sum of cloud liquid water, cloud ice, rain, and snow in ERA5 data is used as the cloud water content. The method of using CloudSat cloud observation data to diagnose cloud area and typical value of cloud water content in the original scheme is replaced. Moreover, the calculation method of condensation and evaporation in the cloud is optimized, the amount of condensation (evaporation) per unit time is improved from the original grid point column to the layered integral, and the amount of condensation and evaporation per unit time are counted. Through comparison and verification, it can effectively improve the underestimation caused by the mutual offset of condensation and evaporation between vertical layers. In this study, ERA5 data can be used for analysis and study from 2011 to 2021. The four seasons in this study are defined as follows: winter (December to February of the next year), spring (March to May), summer (June to August), and autumn (September to November). The definition and calculation methods of the main physical quantities are given as follows [15,40,45,46].

- (1) The gross mass of water vapor: all incoming water vapor participating in the atmospheric water cycle process in the region during a certain evaluation period. The gross mass of water vapor (GM_v) includes the initial water vapor mass (M_{v1}), the annual water vapor inflow (Q_{vi}), the surface evaporation (E_s), and the evaporation from hydrometeors to water vapor (C_{hv}). The calculation formula is as follows:

$$GM_v = M_{v1} + Q_{vi} + E_s + C_{hv} \quad (1)$$

- (2) The gross mass of hydrometeors: all incoming hydrometeors participating in the atmospheric water cycle process in the region during a certain evaluation period. The gross mass of hydrometeors (GM_h) includes the initial hydrometeor mass (M_{h1}), the annual hydrometeor inflow (Q_{hi}), and the condensation from water vapor to hydrometeors (C_{vh}). The calculation formula is as follows:

$$GM_h = M_{h1} + Q_{hi} + C_{vh} \quad (2)$$

- (3) Precipitation: the average precipitation of each grid point in the region is multiplied by the sum of the grid area during a certain evaluation period.
- (4) Cloud water resource: there is no part of surface precipitation in the total cloud water in the region during a certain evaluation period, that is, the cloud water resource

that may be developed by artificial precipitation enhancement technology. Cloud water resource (CWR) includes GM_h and precipitation (P_s). The calculation formula is as follows:

$$CWR = GM_h - P_s \tag{3}$$

- (5) The gross mass of atmospheric water material: the balance equation for the atmospheric water material, which is the summation of water vapor and hydrometeors. The gross mass of atmospheric water material (GM_w) includes GM_v , GM_h . The calculation formula is as follows:

$$GM_w = GM_v + GM_h \tag{4}$$

- (6) The water vapor balance equation is used to calculate C_{vh} and C_{hv} in the cloud: the net condensation ($C_{vh} - C_{hv}$) includes M_{v1} , Q_{vi} , and E_s , the final water vapor mass (M_{vf}), and the annual water vapor outflow (Q_{vo}). The calculation formula is as follows:

$$C_{vh} - C_{hv} = M_{v1} + Q_{vi} + E_s - M_{vf} - Q_{vo} \tag{5}$$

When $(C_{vh} - C_{hv}) > 0$, it is defined as the condensation amount per unit time of the grid point column; otherwise, it is defined as the evaporation amount.

3. Results

3.1. Overall Situation of Atmospheric Water Resources

The multiyear average atmospheric cloud water resources and their conversion efficiency in the Huaihe River Basin from 2011 to 2021 are shown in Tables 1 and 2. In general, the annual average GM_v per unit area in the Huaihe River Basin is approximately 23,201.1 mm, accounting for 93.8% of GM_w . GM_h is approximately 1537.3 mm, accounting for only 6.2% of GM_w , approximately 963.5 mm of P_s falls to the ground, and the average annual PE_h is 62.4% (Table 2). CWR is approximately 573.8 mm.

Table 1. Average annual atmospheric water resources per unit area in the Huaihe River Basin from 2011 to 2021 (unit: mm).

	M_{v1}	M_{h1}	Lateral Boundary			C_{vh}	C_{hv}	P_s	E_s	Total
			Input	Output	Net Input					
Water vapor	5.6		22,102.5	22,045.6	56.9					23,201.1
Cloud water		91.9	295.8	306.6	-10.8	1149.6		963.5		1537.3
Water material			22,398.3	22,352.2	46.1					24,738.4

Table 2. Conversion efficiency of average annual resources in the Huaihe River Basin from 2011 to 2021. CH_v = conversion efficiency from water vapor to hydrometeor. PE_h refers to the average annual PE_h ($PE_h = P_s/GM_h$).

Evaluation Amount	Unit (%)	Remark
CH_v	6.6	GM_h/GM_v
PE_h	62.4	The average annual PE_h

According to the budget conditions (Table 1), the advection transport of water vapor in the Huaihe River Basin is approximately 70 times that of hydrometeors. Most of the water vapor over the river basin is transported horizontally, and the rest is transformed from generation to extinction within the region. For example, the proportion of condensation into cloud water or E_s is very low. The hydrometeor exchanges with each other in the region, which occurs from generation to extinction. The number of hydrometeors generated by atmospheric motion condensation (sublimation) in the region accounts for approximately 79.5% of the total. The proportion of horizontal transport is relatively small. From the

lateral boundary budget condition (Table 1), the annual average net output of hydrometeors per unit area is approximately 10.8 mm.

To verify the rationality of the diagnostic quantification of CWRs in the Huaihe River Basin in this paper, the results are compared with the evaluation results of the six regions (Huaihe River Basin is classified as the central region) in the country in the references [40]. The evaluation values of GM_h (1464.4 mm), P_s (992.4 mm), CWR (472 mm), and PE_h (67.7%) in the central region of reference are the closest to the research results in the Huaihe River Basin [40]. The results show that the diagnostic quantification of CWR and its related quantities in the Huaihe River Basin is reasonable.

The annual average of the water vapor boundary budget per unit area in the Huaihe River basin from 2011 to 2021 is shown in Table 3. The water vapor in the Huaihe River Basin is mainly characterized by the net inflow of the southern boundary and the western boundary and the net outflow of the northern boundary and the eastern boundary. There are two main transportation paths for the net inflow of water vapor: on the one hand, the southwest airflow from the Bay of Bengal flows through the northern Indochina Peninsula into South China and is then transported to the Huaihe River Basin; on the other hand, the southerly airflow formed by the easterly airflow from the south side of the western Pacific subtropical high turning in the South China Sea enters South China and is then transported northward [47]. Water vapor advection transport exhibits obvious seasonal variation. In summer, the water vapor advection transport at each boundary and the overall net incoming water vapor are the largest. In winter, the net inflow of water vapor from the north increases. The overall water vapor budget of each boundary is basically flat. The overall water vapor budgets in spring and autumn are negative.

Table 3. Average annual water vapor boundary budget per unit area in the Huaihe River Basin from 2011 to 2021 (unit: mm).

	East	West	South	North	Whole
Spring	−1792.2	1493.0	614.2	−358.5	−43.5
Summer	−2061.8	1604.1	2216.0	−1634.6	123.7
Autumn	−1569.8	1527.2	215.6	−195.9	−23.0
Winter	−1323.2	1128.5	188.0	6.4	−0.3
Year	−6747.0	5752.9	3233.7	−2182.6	57.0

Table 4 shows the annual average of the hydrometeor boundary budget conditions in the Huaihe River basin. The hydrometeor advection transport in the Huaihe River Basin is a net inflow at the southern and western boundaries throughout the year and four seasons and a net outflow at the northern and eastern boundaries. The seasonal characteristics of hydrometeor transport at each boundary are not obvious. However, there are obvious seasonal characteristics of the hydrometeor budget in the river basin. The whole hydrometeor budget in spring, summer, and autumn is negative; among them, the net output of hydrometeors in summer is the largest. In winter, the whole hydrometeor budget of each boundary is basically flat.

Table 4. Annual average of the hydrometeor boundary budget per unit area in the Huaihe River Basin from 2011 to 2021 (unit: mm).

	East	West	South	North	Whole
Spring	−44.5	36.5	21.9	−14.9	−0.9
Summer	−51.0	40.3	21.8	−19.9	−8.8
Autumn	−40.6	39.8	18.4	−18.9	−1.3
Winter	−33.6	25.5	18.7	−10.5	0.2
Year	−169.7	142.1	80.9	−64.2	−10.9

3.2. Spatiotemporal Distribution Characteristics of CWRs

3.2.1. Interannual Variation Characteristics

Figure 4 shows the interannual variation in CWR and its related quantities (including CWR, Q_{hi} , C_{vh} , P_s , GM_h , and PE_h) in the Huaihe River Basin from 2011 to 2021. Zhou et al. [40] noted that when the study period exceeds a month, the contribution of M_{h1} to GM_h will be less than 1%. For the quantification of CWR in large areas, C_{vh} has the highest contribution to GM_h . Therefore, the interannual variation characteristics of GM_h , C_{vh} , and P_s are relatively consistent.

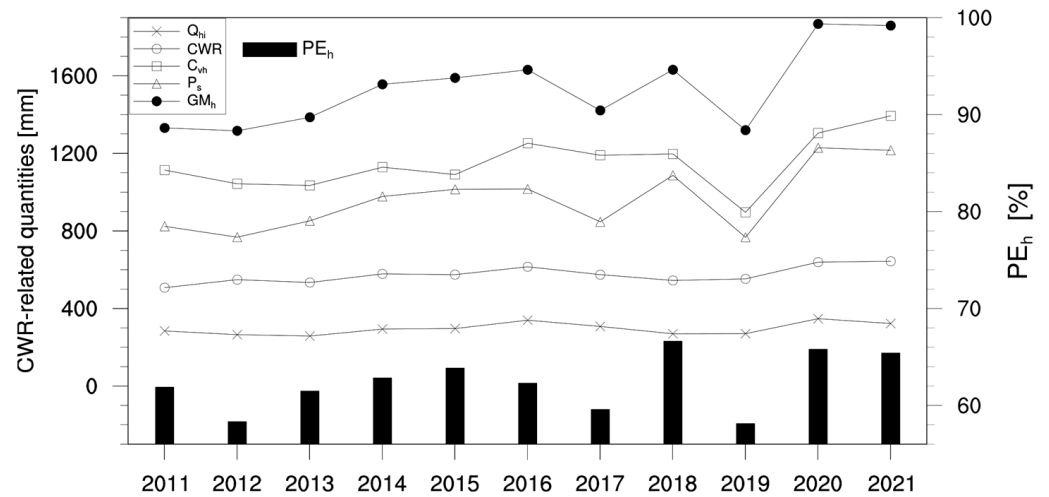


Figure 4. Interannual variation in CWR and its related quantities in the Huaihe River Basin from 2011 to 2021. Q_{hi} = hydrometeor inflow; CWR = cloud water resource; C_{vh} = water vapor converted from hydrometeors through evaporation and sublimation; P_s = surface precipitation; GM_h = the gross mass of hydrometeor; PE_h = precipitation efficiency of hydrometeor.

The CWR in the Huaihe River Basin slowly increased from 2011 to 2021 (between 500 and 650 mm). According to Figure 3, the CWR is the lowest value in 2011 (507.5 mm) and the most abundant in 2021 (643.3 mm). In 2021, the precipitation in the Huaihe River Basin is more than 32%, but the GM_h is also large, so the CWR is also high. Further analysis of CWR and its related quantities shows that the total annual C_{vh} (between 900 and 1400 mm) is the highest, and the annual P_s (between 750 and 1200 mm) is slightly smaller than C_{vh} . The annual Q_{hi} from the boundary of the river basin is significantly less than C_{vh} and P_s , with values between 250 and 350 mm. The annual P_s in 2012 and 2019 in the Huaihe River Basin was less than 800 mm. In 2019, the value was the lowest in the past 10 years (only 767 mm). The main reasons are the serious drought in the Huaihe River Basin in 2012 and the continuous drought in summer and autumn in 2019. In general, the variable C_{vh} is also high and low in the more-rain years and less-rain years, respectively. PE_h has fluctuated between 58% and 67% in the past 10 years; the variation trend is not obvious. After 2016, the interannual variation in GM_h in the Huaihe River Basin became obvious and was very abundant in 2020 and 2021 but relatively small in 2012 and 2019.

3.2.2. Annual Variation Characteristics

To further understand the variation characteristics of CWR and its related quantities, the monthly variation in the multiyear average CWR and its related quantities in the Huaihe River basin were studied (as shown in Figure 5). The monthly variation trends in P_s , CWR, and PE_h are consistent, showing a single-peak distribution, reaching the peak in July and August in midsummer and the lowest in December in winter. The variable PE_h is the highest in August (75.3%). The monthly variation in the proportion of cloud water resource (C_s) is opposite that of P_s , CWR, and PE_h , with the highest C_s in January and the lowest C_s in August. The conversion efficiency of water vapor to hydrometeor

(CH_v) has no obvious seasonal variation. The monthly variation in hydrometeor is mainly caused by the variation in precipitation. PE_h in summer by convective precipitation is significantly higher than that in other seasons, while the PE_h in autumn, winter, and spring are relatively low. Therefore, there is greater potential for artificial development. The precipitation efficiency of hydrometeors can be improved by catalysis technology of artificial precipitation enhancement to increase precipitation.

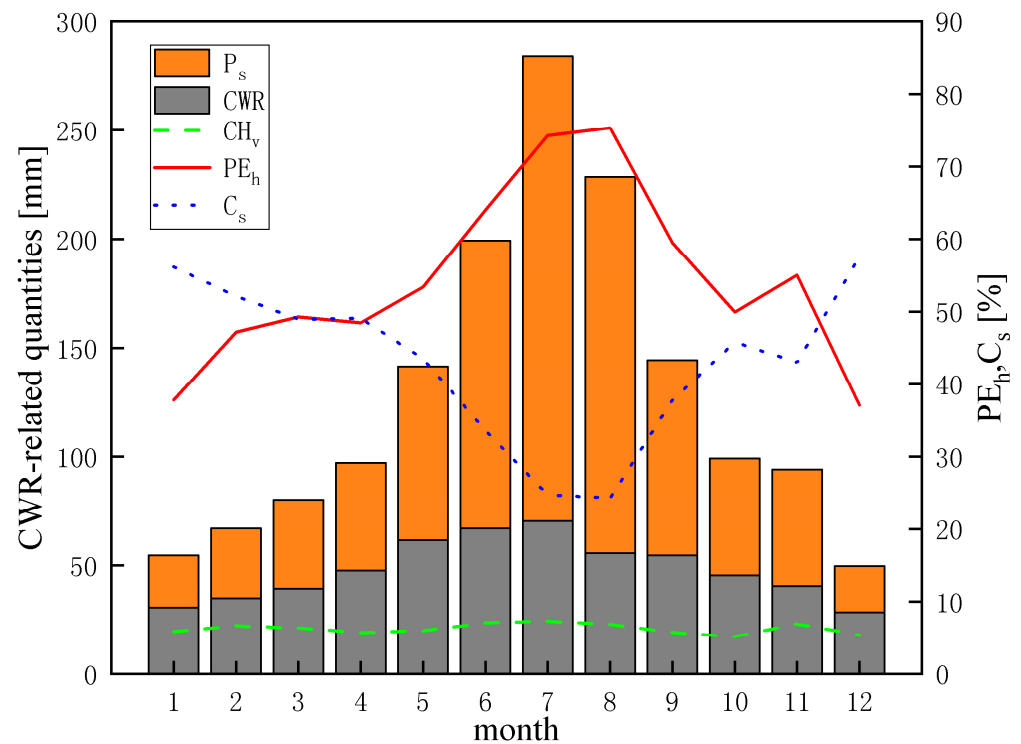


Figure 5. Monthly variation in the multiyear average CWR and its related quantities in the Huaihe River Basin from 2011 to 2021. CH_v = conversion efficiency from water vapor to hydrometeor (green); C_s = proportion of cloud water resources ($C_s = CWR/GM_h$, blue); the related quantities of P_s (orange), CWR (gray), and PE_h (red) are the same as in Figure 2.

3.3. Spatial Distribution Characteristics of CWRs

3.3.1. Horizontal Distribution Characteristics

To further study the distribution characteristics of CWR in the Huaihe River Basin, in this paper, the spatial distributions of GM_v , GM_h , and P_s are analyzed and studied from 2011 to 2021 (as shown in Figure 6). We have found that the distributions of GM_v , GM_h , and P_s are consistent, and the values are zonally distributed and decrease with increasing latitude. The high value area of GM_v is in the southern part of the middle and upper areas of the Huaihe River mainstream, and the highest value reached 330 kg/m^2 , while the low value area is in northern Yishusi, and the lowest value reached 240 kg/m^2 . The high value of GM_h is in the Dabie Mountains in the southern part of the Huaihe River Basin, and the highest value reached 3.4 kg/m^2 , while the low value is in the northern part of the river basin, and the lowest value reached 2.0 kg/m^2 . The spatial distribution of annual P_s is uneven, and the difference between north and south is almost 1.5 times. The high value area is in the southern Dabie Mountains, and the highest value reached 1400 mm, while the low value area is in the northwest of the river basin, and the lowest value reached 800 mm.

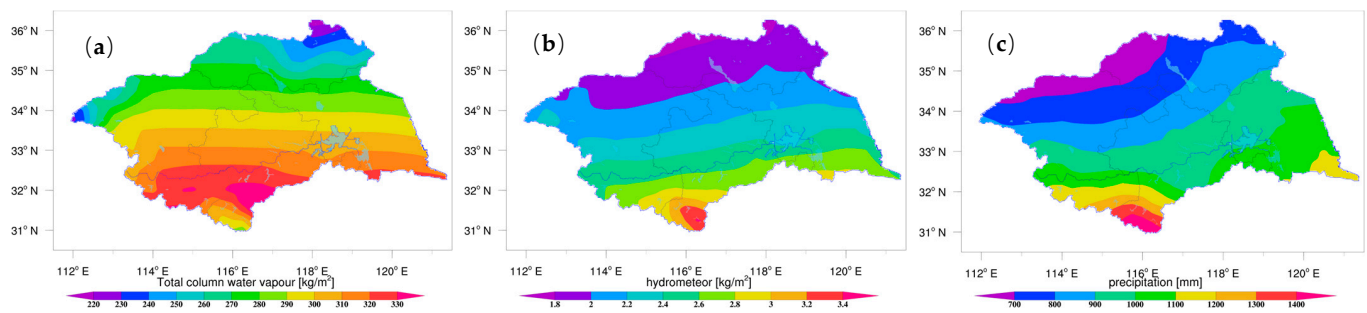


Figure 6. Spatial distribution of CWRs in the Huaihe River basin from 2011 to 2021: (a) GM_V ; (b) GM_H ; (c) annual P_s .

3.3.2. Vertical Distribution Characteristics

Figure 7 shows the vertical distribution of zonal and meridional annual average hydrometeors in the Huaihe River Basin from 2011 to 2021. We first create vertical profiles along the meridional and zonal directions, and then, the spatial average of the grid points in the Huaihe River Basin is obtained along the zonal and meridional directions. Finally, the annual average zonal and meridional vertical distributions of hydrometeors in the Huaihe River Basin are obtained. According to Figure 7a,b, below the 0 °C layer, the warm cloud is mainly composed of liquid water droplets, and the largest values reached 0.48–0.52 g/kg. Above the 0 °C layer, there is a high-value area of hydrometeors between 600 and 400 hPa, and its temperature is between −25 and 0 °C. It is mainly mixed cold hydrometeors composed of liquid phase supercooled droplets and ice phase particles, and the largest value can reach 0.36–0.44 g/kg. Therefore, the large value area of the zonal and meridional vertical distribution of hydrometeors in the Huaihe River Basin mainly appears between 925 and 500 hPa, with the highest value reaching 0.59 g/kg.

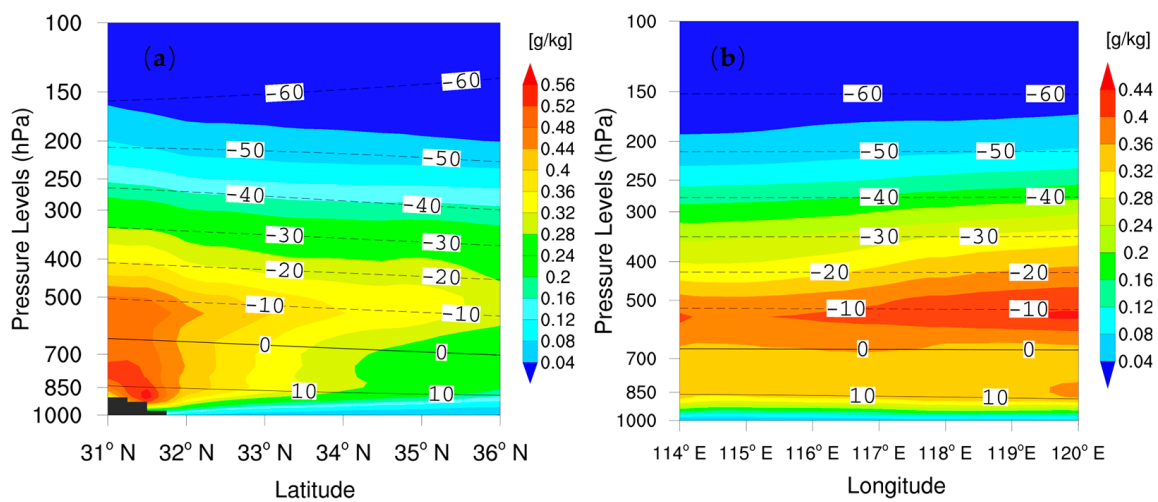


Figure 7. Vertical distribution of zonal (a) and meridional (b) annual average hydrometeors in the Huaihe River Basin from 2011 to 2021. The contour lines (black) denote the temperature.

According to the above analysis, we can see that the horizontal distribution of hydrometeors in the Huaihe River Basin is mainly zonally distributed high in the south and low in the north, and the vertical distribution of hydrometeors shows the characteristics of a high value area between 925 and 500 hPa. To further understand the vertical distribution of hydrometeors in the Huaihe River Basin in different seasons, according to Figure 8, we first create the vertical profiles along the meridional directions, and then, the spatial average of the grid points is obtained along the zonal directions. Finally, the four seasons’ average zonal vertical distribution of hydrometeors in the Huaihe River Basin is

obtained. The distributions of hydrometeors in spring, autumn, and winter are similar. The hydrometeors are mainly distributed in the middle and low levels below 500 hPa (approximately 0.06–0.14 g/kg), with distribution characteristics that are high in the south and low in the north. The hydrometeors in the middle and high levels above 500 hPa are relatively low, basically below 0.04 g/kg, and nearly zero in winter. The vertical distribution characteristics of hydrometeors in summer are completely different from those in spring, autumn, and winter. Hydrometeors are mainly distributed in the middle layer between 600 and 350 hPa (temperature range from -30 to -5 °C), approximately 0.08–0.16 g/kg, while the hydrometeor value and range in the lower layer are significantly reduced. In addition, the high value area of hydrometeors is in the Dabie Mountains. Due to the complex terrain in this area, it is significantly affected by local terrain forcing, and clouds and rain are easily generated. This result is consistent with the horizontal distribution characteristics of the CWRs.

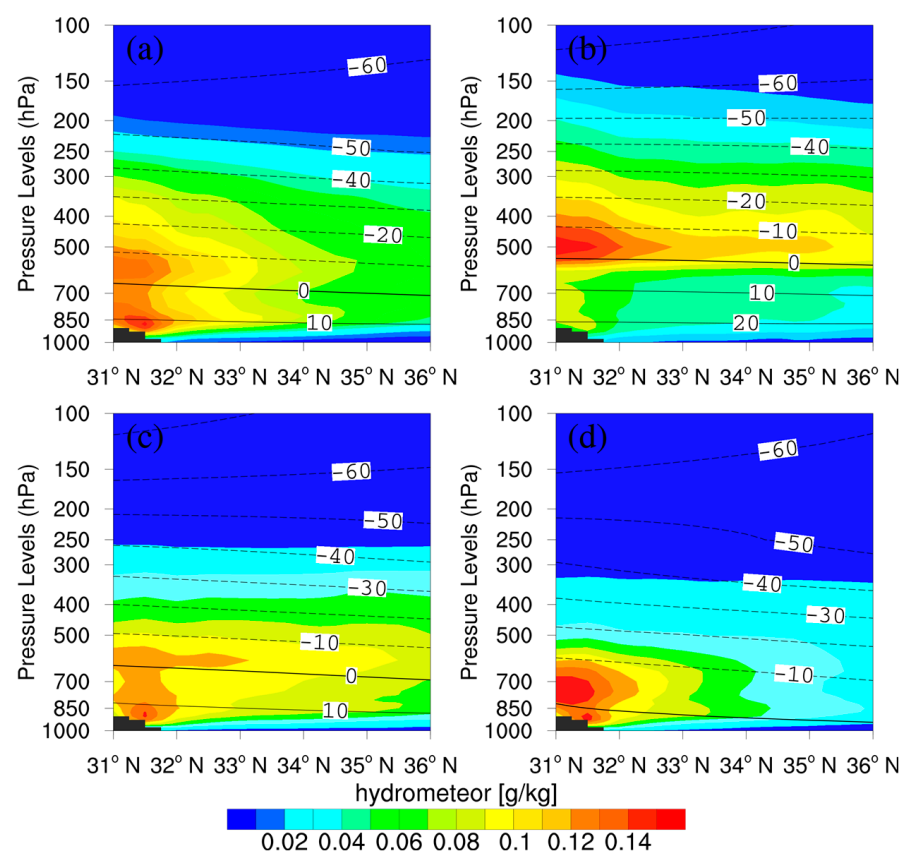


Figure 8. Vertical distribution of the four seasons' average zonal hydrometeors in the Huaihe River Basin from 2011 to 2021. (a–d) represents spring, summer, autumn, winter. The contour lines (black) denote the temperature.

3.4. Comparison of Typical Case Evaluation Results

Based on the above analysis, there are significant differences in the variation characteristics of the CWRs in different seasons in the Huaihe River Basin. Two typical precipitation cases in summer and winter are selected, and a comparative evaluation and analysis of the CWRs are carried out for two cases in the Huaihe River Basin, in which these cases last for 5 days.

On 23–28 June 2000, the Huaihe River Basin was affected by a 500 hPa upper trough and 850 hPa southwest jet stream, and the western Pacific subtropical high extended westward and strengthened northward. Furthermore, with low-level shear, the cold and warm air converged and was maintained in the region, which provided favorable conditions for the convective precipitation weather process in the Huaihe River Basin. As seen

from the vertical distribution of zonal and meridional hydrometeors at 7:00 BJT (Beijing time, the same as below) on 26 June (the strongest moment of the process, Figure 9a,b), hydrometeors were in the northern and central regions, respectively. The distribution of hydrometeors mainly appeared between 600 and 200 hPa, mainly cold clouds, and fewer hydrometeors appeared below 600 hPa. This result is consistent with the vertical distribution characteristics of hydrometeors in the Huaihe River Basin in summer. On 1–6 December 2018, the Huaihe River Basin was affected by the 500 hPa upper trough and the low-level shear. Moreover, 850 hPa southerly airflow provided water vapor transport for the region, which was a typical stratiform cloud precipitation case in the Huaihe River Basin in winter. As seen from the vertical distribution of zonal and meridional hydrometeors at 19:00 BJT on 5 December (the strongest moment of the case), hydrometeors were in the southern and eastern regions, respectively (Figure 9c,d). The hydrometeors were mainly distributed between 925 and 500 hPa, with cold and warm clouds. There were mainly warm clouds south of 32°N, and the 0 °C layer dropped to 700 hPa, with cold clouds. There were basically no hydrometeors above 500 hPa. The above analysis results are consistent with the vertical distribution characteristics of hydrometeors in the Huaihe River Basin in winter.

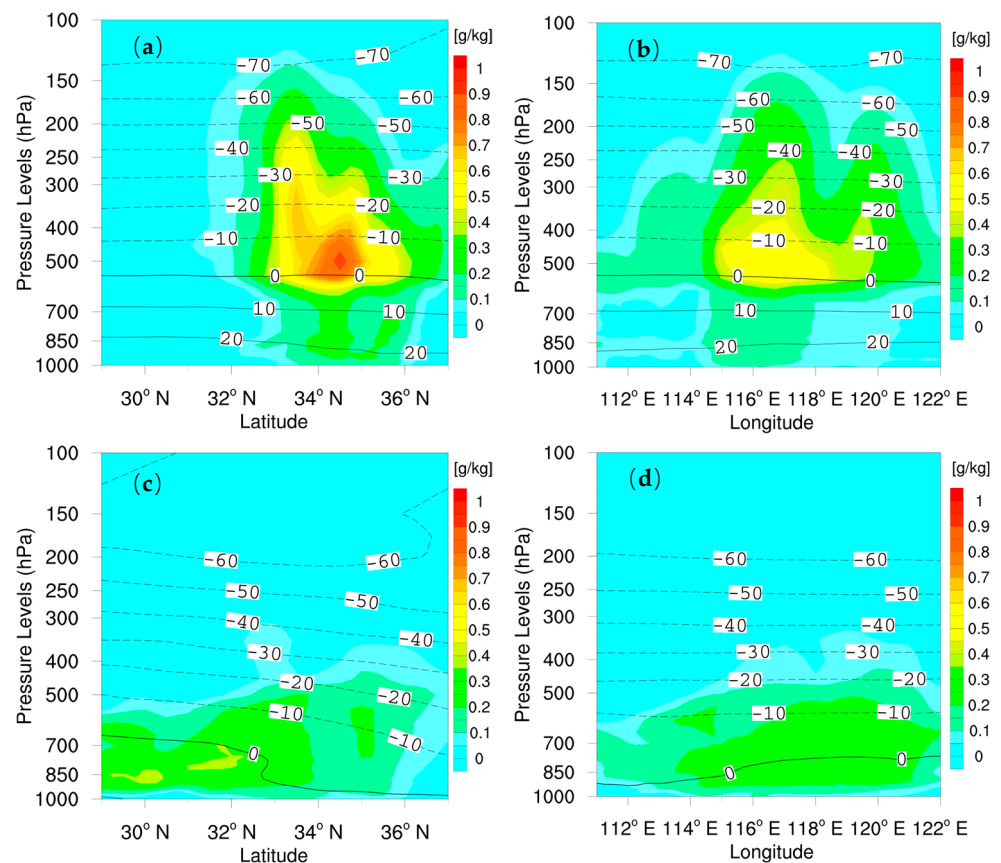


Figure 9. Vertical distribution of zonal and meridional hydrometeors in different types of clouds of two cases: summer ((a,b); at 7:00 BJT on 26 June 2000) and winter ((c,d); at 19:00 on 5 December 2018). The contour lines (black) denote the temperature.

Comparative evaluation and analysis of the CWRs are conducted for two different types of precipitation weather cases in winter and summer in the Huaihe River Basin. According to Table 5, there are differences in the variation characteristics of the CWRs between the two cases in the following respects: (1) The amount of water vapor in the summer case is significantly higher than that in winter, which can provide better water vapor conditions for the formation of cloud water. (2) GM_v in the summer case is nearly 2 times that in winter, and although the summer CH_v was slightly higher than that of the

stratiform cloud case, M_{h1} , M_{hf} , Q_{hi} , and the lateral boundary hydrometeor output (Q_{ho}) of the two cases are basically the same, and the differences in C_{vh} , GM_h , and P_s are almost 3 times. (3) The GM_h in the convective cloud case is more than 3 times that in the stratiform cloud case, and the P_s is more than 4 times that in the stratiform cloud case. According to the calculation formula of CWR ($CWR = GM_h - P_s$), the CWR in the two precipitation cases in summer and winter are similar. However, PE_h in the convective cloud case is significantly higher than that in the stratiform cloud case.

Table 5. Comparative evaluation of precipitation cases in summer and winter.

Physical Quantities of Atmospheric Water Resources		Summer Case	Winter Case
water vapor mm	initial value	43.3	23.1
	input	907.8	343.7
	final value	65.1	9.8
	output	786.1	335.2
	GM_v	962.7	375.6
cloud water mm	initial value	0.1	0.3
	input	9.7	10.2
	final value	0.7	0.2
	output	13.9	11.6
	condensation GM_h	111.6 139.0	30.6 45.0
precipitation mm	P_s	122.5	29.1
conversion efficiency %	CH_v	14.4	12.0
	PE_h	88.1	64.7
cloud water resource mm		16.5	15.9

4. Discussions

- (1) Due to the coarse grid resolution of regional grid decomposition, the evaluation accuracy of the quantitative evaluation method of CWRs in any region is reduced. In the future, reanalysis data can be downscaled by using the super resolution technology of artificial intelligence or the dynamic downscaling technology of regional numerical models to calculate the regional CWRs at finer grids (such as 10 km and 5 km) and reduce the evaluation errors caused by a coarse grid resolution.
- (2) As a product of data assimilation, there are some characteristics of uniform spatial distribution, longtime scale, and continuity of data for reanalysis. It is an effective way to study CWRs. However, different atmospheric reanalysis data may impact the results. In the future, more atmospheric reanalysis data can be used for the calculation and comparative analysis of CWR quantification.

5. Conclusions

Based on the ERA5 reanalysis data and gridded observed precipitation data, combined with the CWR-DQ method released by the weather modification center of the China Meteorological Administration, we have analyzed and evaluated the CWRs and their distribution characteristics in the Huaihe River Basin from 2011 to 2021. Furthermore, the CWRs of two typical precipitation cases in summer and winter have been compared and evaluated.

- (1) From the multiyear average, the annual GM_h of the Huaihe River Basin is 4721.4 billion tons (the regional average is approximately 1537.3 mm); among them, the annual P_s is 2586.7 billion tons (963.5 mm), the CWR is 1540.7 billion tons (573.8 mm), and the average annual PE_h is 62.4%. The hydrometeors exchange with each other in the

- region, which occurs from generation to extinction. The annual average net output of hydrometeors is approximately 29.2 billion tons (10.8 mm).
- (2) The CWR in the Huaihe River Basin shows a slow increasing trend from 2011 to 2021, while PE_h is not obvious. CWR was the lowest in 2011 (507.5 mm) and the most abundant in 2021 (643.3 mm). The annual P_s was the lowest in 2019 (767.0 mm) and the highest in 2020 (1228.9 mm). C_{vh} is high in the rainier years and low in the less rainy years. The monthly variations in P_s , CWR, and PE_h show a single peak distribution. CH_v has no obvious seasonal variation. PE_h in summer is significantly higher than that in other seasons.
 - (3) The spatial horizontal distributions of GM_v , GM_h , and P_s in the Huaihe River Basin are zonal, and the values decrease with increasing latitude. The high value area of the vertical distribution of hydrometeors in the river basin is mainly between 925 and 500 hPa in the southeast of the river basin. Below the 0 °C layer, the warm cloud is mainly composed of liquid water droplets. Above the 0 °C layer, between 600 and 400 hPa, there are mainly mixed cold hydrometeors composed of liquid phase supercooled droplets and ice phase particles. In summer, the vertical distribution of hydrometeors is relatively high, between 600 and 350 hPa, with fewer hydrometeors at low levels. The hydrometeors in spring, autumn, and winter are mainly below 500 hPa.
 - (4) Based on a comparison of the CWRs between summer and winter precipitation cases, the GM_v , C_{vh} , CWR, P_s , and PE_h in summer are significantly higher than those in winter. GM_h in the convective cloud case is more than 3 times that in the stratiform cloud case; the P_s is more than 4 times that in the stratiform cloud case. The CWRs of the two precipitation cases in summer and winter are similar. PE_h in the convective cloud case is significantly higher than that in the stratiform cloud case.

The study results are helpful to propose rational suggestions in the Huaihe River Basin and to provide some theoretical basis for the development of CWRs. In fact, in the operation of artificial precipitation enhancement, we should comprehensively evaluate the potential of precipitation enhancement, such as water vapor and hydrometeor and precipitation efficiency, and adopt suitable catalytic methods to achieve a better artificial precipitation enhancement effect.

Author Contributions: Conceptualization, J.G. and Y.C.; Data curation, J.F. and X.Z.; Formal analysis, J.G. and Y.C.; Methodology, J.G. and Y.C.; Investigation, J.G., Y.C. and J.F.; Writing—original draft, J.G.; Writing—review and editing, Y.C., J.F. and X.Z. All authors have read and agreed to the published version of the manuscript.

Funding: This research was funded by the National Key Research and Development Program of China, grant number 2019YFC1510303; Anhui Province Key Research and Development Plan Project, China, grant number 1704f0804055.

Institutional Review Board Statement: Not applicable.

Informed Consent Statement: Not applicable.

Data Availability Statement: The data are available on request.

Acknowledgments: We thank the European Center for Medium-Range Weather Forecasts (ECMWF) for providing ERA5 reanalysis datasets.

Conflicts of Interest: The authors declare no conflict of interest.

References

1. Gupta, N.; Bearup, L.; Jacobs, K.; Halper, E.; Castro, C.; Chang, H.-I.; Fonseca, J. Stakeholder-Informed hydroclimate scenario modeling in the lower Santa Cruz River Basin for water resource management. *Water* **2023**, *15*, 1884. [[CrossRef](#)]
2. Girma, A.; Yan, D.; Wang, K.; Birara, H.; Gedefaw, M.; Batsuren, D.; Abiyu, A.; Qin, T.; Mekonen, T.; Abate, A. Climate Change, Land Use, and Vegetation Evolution in the Upper Huai River Basin. *Atmosphere* **2023**, *14*, 512. [[CrossRef](#)]
3. Chen, F.J.; Hao, H. Comparisons of Gauge, TMPA and IMERG products for Monsoon and Tropical Cyclone Precipitation in Southern China. *Pure Appl. Geophys.* **2019**, *176*, 1767–1784. [[CrossRef](#)]

4. Yu, X.J.; Zhang, L.X.; Zhou, T.J.; Zheng, X. Long-term changes in the effect of drought stress on ecosystems across global drylands. *Sci. China Earth Sci.* **2023**, *66*, 146–160. [[CrossRef](#)]
5. Yao, R.; Xia, M.; Sun, P.; Wen, Q.Z.; Liu, G.N.; Liang, Y.Y. Spatio-temporal distribution characteristics of meteorological drought and climate influence factors. *Acta Ecol. Sin.* **2021**, *41*, 333–347.
6. Chen, S.J.; Ju, Q.; Hao, Z.C.; Wang, L.Y.; Xu, H.Q. Analysis of extreme hydrometeorological characteristics in Huaihe River Basin in recent 70 years. *J. Hebei Univ. Eng.* **2020**, *37*, 75–83.
7. Manatsa, D.; Mushore, T.; Lenouo, A. Improved predictability of droughts over southern Africa using the standardized precipitation evapotranspiration index and ENSO. *Theor. Appl. Climatol.* **2015**, *127*, 259–274. [[CrossRef](#)]
8. Chen, F.J.; Fu, Y.F.; Yang, Y.J. Regional Variability of precipitation in Tropical Cyclones over the Western North Pacific Revealed by the GPM Dual-Frequency Precipitation Radar and Microwave Imager. *JGR Atmos.* **2019**, *124*, 11286–11296.
9. Farooq, U.; Taha Bakheit Taha, A.; Tian, F.; Yuan, X.; Ajmal, M.; Ullah, I.; Ahmad, M. Flood Modelling and Risk Analysis of Cinan Feizuo Flood Protection Area, Huaihe River Basin. *Atmosphere* **2023**, *14*, 678. [[CrossRef](#)]
10. Wang, S.; Tian, H.; Xu, M.; Xie, W.S.; Tao, Y. Analysis of extreme precipitation events in rainy season over Huaihe River Basin from 1961 to 2008. *Meteorol. Sci. Technol.* **2012**, *40*, 87–91.
11. Chen, W.L.; Jiang, Z.H.; Huang, Q. Projection and simulation of climate extremes over the Yangtze and Huaihe River basins based on a statistical downscaling model. *Trans. Atmos. Sci.* **2012**, *35*, 578–590.
12. Pan, X.; Yin, Y.X.; Wang, X.J. Spatio-temporal characteristics of the occurrence timing of extreme precipitation in the Huai River basin from 1960 to 2014. *Plateau Meteorol.* **2019**, *38*, 377–385.
13. Lu, Y.Y.; Wu, B.W.; Tian, H.; Sun, W. Spatial and temporal variability characteristics of precipitation in Huai River during 1961–2005. *Resour. Environ. Yangtze Basin* **2011**, *20*, 567–573.
14. Jin, H.; Chen, X.; Zhong, R.; Pan, Y.; Zhao, T.; Liu, Z.; Tu, Y. Spatiotemporal distribution analysis of extreme precipitation in the Huaihe River Basin based on continuity. *Nat. Hazards* **2022**, *114*, 3627–3656.
15. Zhang, Z.G.; Jian, Y.; Li, Y.Z.; Zhan, Y.Y. Assessment of cloud water resources of Guangxi based on ERA5 data. *Meteorol. Sci. Technol.* **2021**, *49*, 806–814.
16. Chen, Y.H.; Huang, J.P.; Chen, C.H.; Zhang, Q.; Feng, J.D.; Jin, H.C.; Wang, T.H. Temporal and spatial distribution of cloud water resources over Northwestern China. *Plateau Meteorol.* **2005**, *24*, 905–912.
17. Lin, D. Temporal and spatial distribution and change trend of cloud water of different types clouds in Southwest China. *J. Arid Meteorol.* **2015**, *33*, 748–755.
18. Liu, H.L.; Zhu, W.Q.; Yi, S.H.; Chen, L.X.; Bai, L.J. Climatic analysis of the cloud over China. *Acta Meteorol. Sin.* **2003**, *61*, 466–473.
19. Li, X.Y.; Guo, X.L.; Zhu, J. Climatic distribution features and trends of cloud water resources over China. *Chin. J. Atmos. Sci.* **2008**, *32*, 1094–1106.
20. Liu, J.J.; You, Q.L.; Wang, N. Interannual anomaly of cloud water content and its connection with water vapor transport over the Qinghai-Tibetan Plateau in summer. *Plateau Meteorol.* **2019**, *38*, 449–459.
21. Sun-Mack, S.; Minnis, P.; Chen, Y.; Gibson, S.; Yi, Y.H.; Trepte, Q.; Wielicki, S.; Kato, S.; Winker, D.; Stephens, G.; et al. Integrated cloud-aerosol-radiation product using CERES, MODIS, CALIPSO, and CloudSat data. *Terms Use* **2007**, *6745*, 674513.
22. Tian, J.J.; Dong, X.Q.; Xi, B.K.; Minnis, P.; Smith, W.L., Jr.; Sun-Mack, S.; Thieman, M.; Wang, J. Comparisons of ice water path in deep convective systems among ground-based, GOES, and CERES-MODIS retrievals. *J. Geophys. Res. Atmos.* **2018**, *123*, 1708–1723.
23. Zhou, Y.Q.; Ou, J.J. The method of cloud vertical structure analysis using rawinsonde observation and its applied research. *Meteorol. Mon.* **2010**, *36*, 50–58.
24. Wang, S.H.; Han, Z.G.; Yao, Z.G.; Zhao, Z.L. An analysis of cloud types and macroscopic characteristics over China and its neighborhood based on the CloudSat data. *Acta Meteorol. Sinica* **2011**, *69*, 883–899.
25. Cai, M. Cloud Water Resources and Precipitation Efficiency Evaluation over China. Ph.D. Thesis, Chinese Academy of Meteorological Sciences, Beijing, China, 2013; pp. 1–124.
26. Zhao, H.Y.; Jiang, H.; Wang, K.L.; Yu, Y.X.; Yang, Y.F. The atmospheric water resource over the Qilian-Heihe Valley. *J. Meteor. Res.* **2006**, *20*, 90–97.
27. Wang, K.L.; Cheng, G.D.; Jing, H.; Zhang, L.J. Atmospheric hydrologic cycle over the Qilian-Heihe Valley. *Adv. Water Sci.* **2003**, *14*, 91–97.
28. Wang, L.J.; Sun, A.P.; Liu, C.H.; Zhao, K. Application of ground-based microwave radiometer detection to precipitation enhancement in the upper of the Yellow River. *Meteorological* **2007**, *33*, 28–33.
29. Zhang, J.; Zhang, Q.; Tian, W.S.; He, J.M. Remote sensing retrieval and analysis of optical character of cloud in Qilian mountains. *J. Glaciology Geocryol.* **2006**, *28*, 722–727.
30. Han, Q.; Rossow, W.; Welch, R.; Chou, J. Validation of satellite retrievals of cloud microphysics and liquid water path using observations from FIRE. *J. Atmos. Sci.* **1995**, *52*, 4183–4195. [[CrossRef](#)]
31. Yang, D.S.; Wang, P.C. Characteristics of vertical distributions of cloud water contents over China during summer. *Chin. J. Atmos. Sci.* **2012**, *36*, 89–101.
32. Bai, L.; Wang, W.X.; Yao, Y.N.; Ma, J.; Li, L.H. Reliability of NCEP/NCAR and ERA-Interim reanalysis data on Tianshan mountainous area. *Desert Oasis Meteorol.* **2013**, *7*, 51–56.
33. Liu, J.J.; You, Q.L.; Zhou, Y.Q.; Ma, Q.R.; Cai, M. Distribution and trend of cloud water content in China based on ERA-Interim reanalysis. *Plateau Meteorol.* **2018**, *37*, 1590–1604.

34. Zhang, H.H.; Shi, M.M.; Hu, H.; Qi, D.L.; Quan, C. Cloud water resources assessment in Qinghai province based on ERA-Interim reanalysis data. *J. Arid Meteorol.* **2021**, *39*, 569–576.
35. Li, W.B.; Zhu, Y.J.; Zhao, B.L. Estimation of cloud liquid water over the HUBEX area using TRMM/TMI. *Acta Meteorol. Sin.* **2003**, *61*, 116–121.
36. Yao, Z.Y.; Wang, G.H.; You, L.G.; Liu, Y.H.; Li, W.B.; Zhu, Y.J.; Zhao, B.L. Microwave remote sensing of cloud liquid water in Shouxian area. *J. Appl. Meteorol. Sci.* **2001**, *12*, 88–95.
37. Li, W.B.; Tong, K.; Gu, S.Y.; Yao, Z.Y.; Liu, W.M.; Gao, H.L.; Zhu, Y.J.; Zhao, B.L.; Liu, H.Z. A study on the application of satellite remote sensing in HUBEX. *Acta Sci. Nat. Univ. Pekin.* **2003**, *39*, 118–124.
38. Cao, Y.N.; Zhou, S.X.; Yuan, Y.; Wu, L.L. Cloud Properties in different regions of Anhui province based on MODIS cloud product. *Remote Sens. Inf.* **2020**, *35*, 53–62.
39. Zheng, X.Y.; Yang, Y.J.; Yuan, Y.; Cao, Y.N.; Gao, J.L. Comparison of macro- and microphysical properties in precipitating and non-Precipitating clouds over Central-Eastern China during warm season. *Remote Sens.* **2022**, *14*, 152. [[CrossRef](#)]
40. Cai, M.; Zhou, Y.Q.; Liu, J.Z.; Tang, Y.H.; Tan, C.; Zhao, J.J.; Ou, J.J. Diagnostic Quantification of the Cloud Water Resource in China during 2000–2019. *J. Meteor. Res.* **2022**, *36*, 292–310. [[CrossRef](#)]
41. ECMWF. IFS Documentation-Cy46r1 (Part IV: Physical Processes) [EB/OL]. Available online: <http://www.ecmwf.int/en/publications/ifs-documentation> (accessed on 22 June 2020).
42. Vásquez Anacona, H.; Mattar, C.G.; Alonso-de-Linaje, N.; Sepúlveda, H.H.; Crisóstomo, J. Wind Simulations over Western Patagonia Using the Weather Research and Forecasting Model and Reanalysis. *Atmosphere* **2023**, *14*, 1062. [[CrossRef](#)]
43. Ma, Y.H.; Mao, R.; Yang, Y.; Ma, L.; Gou, S. Evaluation of the ERA5 Reanalysis Data on the Near-Surface Wind Speed Climate Characteristics and Change Trend Reproduction Ability in Gansu Province. *Plateau Meteorol.* **2023**, *42*, 210–220.
44. Yang, Y.; Wang, L.J.; Huang, X.Y.; Qi, Y.; Xie, R. Analysis on spatio-temporal variation of evapotranspiration in the Yellow River Basin based on ERA5-Land products. *J. Arid Meteorol.* **2023**, *41*, 390–402.
45. Zhou, Y.Q.; Cai, M.; Tan, C.; Mao, J.T.; Hu, Z.J. Quantifying the Cloud Water Resource: Basic Concepts and Characteristics. *J. Meteor. Res.* **2020**, *34*, 1242–1255. [[CrossRef](#)]
46. Cai, M.; Zhou, Y.Q.; Liu, J.Z.; Tan, C.; Tang, Y.H.; Ma, Q.R.; Li, Q.; Mao, J.T.; Hu, Z.J. Quantifying the Cloud Water Resource: Methods Based on Observational Diagnosis and Cloud Model Simulation. *J. Meteorol. Res.* **2020**, *34*, 1256–1270. [[CrossRef](#)]
47. Xu, M.; Tian, H. The relationship between the atmospheric vapor transportation and the rainfall over Huaihe River Basin during the meiyu period in 2003. *Sci. Meteorol. Sin.* **2005**, *25*, 265–271.

Disclaimer/Publisher’s Note: The statements, opinions and data contained in all publications are solely those of the individual author(s) and contributor(s) and not of MDPI and/or the editor(s). MDPI and/or the editor(s) disclaim responsibility for any injury to people or property resulting from any ideas, methods, instructions or products referred to in the content.